Accepted Manuscript

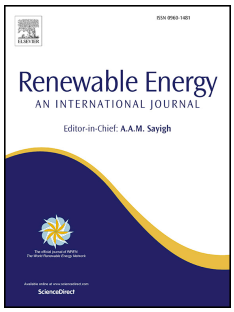

Superposition of the single point source solution to generate temperature response factors for geothermal piles

M. Fossa, A. Priarone, F. Silenzi

PII: S0960-1481(19)30663-9

DOI: https://doi.org/10.1016/j.renene.2019.05.011

Reference: RENE 11603

To appear in: *Renewable Energy*

Received Date: 4 January 2019

Revised Date: 10 April 2019

Accepted Date: 3 May 2019

Please cite this article as: Fossa M, Priarone A, Silenzi F, Superposition of the single point source solution to generate temperature response factors for geothermal piles, *Renewable Energy* (2019), doi: https://doi.org/10.1016/j.renene.2019.05.011.

Superposition of the Single Point Source solution to generate Temperature Response Factors for Geothermal Piles

M. Fossa, A. Priarone, F. Silenzi

Abstract

Geothermal piles are a very promising technique to exploit the low enthalpy resource for ground coupled heat pumps. In fact, they are heat exchangers integrated in the foundation structures of the buildings, with reduced need in term of ground surface availability and diminished drilling costs. Unfortunately, to evaluate the ground thermal response to their presence it is not possible to use classical analytical solutions due to their low aspect ratio and to the relevant effect of the heat capacity of the inner cylindrical volume. In addition, different shapes of the pipe arrangement are possible: helix around the foundation pile or a series of vertical pipes connected through U bends at top and bottom of the cylindrical volume.
This study proposes a semi-analytical method to model ground heat exchangers with a great flexibility concerning their shape. The method, called Multiple Point Sources (MPS), applies the spatial superposition of the analytical solution for the Single Point Source. It has been validated by means of the comparison with literature analytical methods and FEM results for helix heat exchangers. Finally, it has been applied to find the temperature response factor for different shapes of heat exchanger in geothermal piles.

Keywords: Ground coupled heat pumps; geothermal piles; temperature response factors; superposition method.

1. Introduction

Geothermal energy exploitation with Ground Coupled Heat Pump (GCHPs) is a great opportunity for environmental protection and energy saving for both residential and commercial buildings. A typical geothermal system is based on the realization of horizontal or vertical heat exchanger fields. Horizontal ones are very demanding for available surface area whereas vertical borehole heat exchangers (BHE) have very good performance but high initial costs due to the drilling equipment (Holmberg et al., 2016).
For these reasons, short vertical heat exchangers have been developed and studied. Such shallow ground heat exchangers can be integrated directly into the building foundation elements (Ghasemi-Fare and Basu 2016, Jelušič and Žlender 2018). Inside foundation piles (also referred as geothermal piles or energy piles), the heat exchangers can be arranged into helix configurations (Helix Heat Exchangers, HHE), defining a cylindrical volume that is typically filled with steel reinforced concrete.
If geothermal piles are considered, the classical models for vertical BHE (infinite line source ILS, finite line source FLS, infinite cylindrical heat source ICS) become inappropriate to describe the heat exchanger thermal behavior with respect to ground. In fact, due to the reduced depth of the pile, the influence of the heat transfer area at the top and bottom end of the heat exchanger becomes relevant and makes the above “slim” models unsuitable for engineering design. Moreover, the presence of the additional thermal capacity of the concrete volume affects the heat transfer. For these reasons, devoted models have to be developed for such a problem.
One of the first studies dealing with the present topic was the one by Rabin and Korin (1996). They modeled the spiral heat exchanger by means of a series of rings with constant pitch distance and

solved the thermal problem numerically. The results have been compared with data from field experiments considering the effects of the thermal properties of the soil, the aspect ratio of the heat exchanger and its pitch distance. An interesting numerical approach has been recently adopted by Zarrella et al. (2015) who developed a resistance-capacitance thermal model for simulating a HHEs field. They analyzed the effects induced by different geometrical parameters and ground properties (i.e. the effects of axial conduction and of the surface temperature).

Recently, a Chinese research group (Man et al. 2010-2011, Cui et al. 2011) developed a series of analytical solutions based on the Green's function method to represent the thermal response of HHEs into the ground. The proposed models are of growing complexity and they include the infinite and finite "solid" cylindrical geometries (in which ground is assumed to occupy also the inner cylindrical volume), infinite and finite ring and helix source configurations.

Some works combine the conduction heat transfer in the ground with other effects. Moch et al. (2014) numerically solved the soil freezing problem around a helix coil, modelling the HHE as a series of rings or as a finite cylinder filled with ground. Moch and co-workers compared the theoretical results with experimental data, finding satisfactory agreement. Go et al. (2015) investigated the effects of groundwater advection into the ground on the performance of a spiral coils field by numerically solving the conjugate heat transfer problem with the commercial code Comsol Multiphysics.

In this paper, to simulate geothermal piles with spiral and U arranged pipes, a semi-analytical method is proposed, based on the spatial superposition of the analytical solution of the Single Point Source problem (SPS). First, the reliability of the model has been extensively checked in terms of numerical discretization (heat sources density effects), also with a validation against literature analytical solutions. Then, two different geometries of heat exchanger have been considered and modelled: a series of ring coils around a solid cylinder and a series of vertical pipes connected through U bends at top and bottom of a cylindrical volume.

2. Theoretical background

Ground heat exchangers (GHEs) behavior is frequently described in terms of a network of two thermal resistances, the first pertaining to the heat exchanger itself and the second related to the time-dependent response of the ground to the presence of the GHE. To study the ground thermal response it is a common practice to solve the transient conduction equation, to obtain the temperature field as a function of time according to a 1D (radial) or 2D (radial and axial) description of the thermal domain.

Frequently, the temperature field can be represented in a dimensionless form by the introduction of a proper Temperature Response Factor (TRF). Its formulation depends on the applied boundary conditions as discussed in details for example by Priarone and Fossa (2016). A general expression for any TRF solution can be written with reference to the applied heat transfer rate per unit length:

$$\Gamma = \frac{2\pi k_{gr}(T - T_{gr,\infty})}{\dot{Q}} \qquad (1)$$

This basic dimensionless solution, expressed as a function of a proper Fourier number, can be profitably superposed in space and time (Ingersoll et al. 1954, Eskilson 1987), in order to simulate the transient response of a GHE field when subjected to variable thermal loads to the ground (Yavuzturk and Spitler, 1999, Bernier et al. 2004).

The temperature field around the GHE can be obtained through both numerical and analytical approaches.

In the following the main analytical solutions for describing the effects of heat sources buried in the ground are presented and discussed. For all those models the ground is assumed to be an

101 homogeneous medium, with thermo-physical properties not dependent from temperature and initial
102 uniform temperature equal to $T_{gr,\infty}$ in the whole domain.

103

2.1. Analytical solutions for point, line and cylindrical heat sources

A series of simplified geometries have been considered for describing a real ground heat exchanger. They refer to heat sources having different shapes, ranging from the single point configuration, to infinite and finite line and cylindrical sources. This section is devoted to the description of the above geometries (as sketched in Table 1) and to the related analytical solutions to the heat conduction problem.

A very early model for geothermal applications is the Single Point Source (SPS) one, where the source is delivering a constant heat transfer rate $\dot{Q}$. The related SPS solution can be expressed in terms of the complementary error function as:

$$T(r,\tau) = T_{gr,\infty} + \frac{\dot{Q}}{2\pi k_{gr}} \frac{1}{2r} erfc\left(\frac{1}{2\sqrt{Fo_r}}\right) \tag{2}$$

This solution has been the starting point for obtaining further ones for more complex source geometries using the superposition technique.

The first application of the superposition method of the Single Point Source solution has been applied to obtain the Infinite Line Source (ILS) model. The model has been described in details by Ingersoll et al. (1954), following the work of Carslaw and Jager (1947):

$$\Gamma_{ILS}(r,\tau) = 2 \cdot \int_{1/4Fo}^{\infty} \frac{e^{-\beta}}{\beta} d\beta = 2 \cdot E_1\left(\frac{1}{4 \cdot Fo_r}\right) \tag{3}$$

The expression of the ILS solution contains the exponential integral function E_1, that can be evaluated with proper truncated series expansions, including the Abramovitz and Stegun (1964) approximation:

$$E_1 = a_0 - \ln\left(\frac{1}{4Fo_r}\right) + \sum_{j=1}^{5} a_j \left(\frac{1}{4Fo_r}\right)^j \tag{4}$$

where

a_0 = – 0.57721566 a_3 = 0.05519968

a_1 = 0.99999193 a_4 = – 0.2491055

a_2 = – 0.24991055 a_5 = 0.00107857

The above approximated expression of E_1 can be proved to be accurate within 10% if $Fo_r > 0.25$ (i.e. the argument of the exponential integral $(1/4 \cdot Fo_r)$ is smaller than 1) and within 1% if $Fo_r > 2$.

The integration over a line of length H allows to obtain the temperature field at any radial and axial position around the finite line source (in infinite medium) as the superposition in space of multiple point source contributions. Equation (5) shows the result of this integration (present paper contribution), that refers to the Finite Line Source in a Infinite medium (FLSI):

$$\Gamma_{FLSI}(r,z,\tau) = \frac{1}{2} \cdot \int_0^H \left[\frac{erfc\left(\frac{\sqrt{(z-h)^2 + r^2}}{2\sqrt{a\,\tau}}\right)}{\sqrt{(z-h)^2 + r^2}} \right] dh \tag{5}$$

To obtain the solution for the Finite Line Source in a semi-infinite medium (FLS), it is necessary to consider the superposition of a series of image sources of opposite heat rate strength with respect to a plain of symmetry which represents the ground surface, at which the temperature remains constant and equal to the initial undisturbed one, $T_{gr,\infty}$.

For FLS, Zeng et al. (2002) proposed the following solution:

$$\Gamma_{FLS}(r,z,\tau)=\frac{1}{2}\cdot\int_0^H\left[\frac{erfc\left(\frac{\sqrt{(z-h)^2+r^2}}{2\sqrt{a\,\tau}}\right)}{\sqrt{(z-h)^2+r^2}}-\frac{erfc\left(\frac{\sqrt{(z+h)^2+r^2}}{2\sqrt{a\,\tau}}\right)}{\sqrt{(z+h)^2+r^2}}\right]dh \tag{6}$$

Lamarche and Beauchamp (2007) solution provides the excess temperature as a function of radius and time as the average along *z* for a length *H*:

$$\Gamma_{FLS\ ave}(r,\tau)=\left[\int_{\beta}^{\sqrt{\beta^2+1}}\frac{erfc(\gamma\cdot z)}{\sqrt{z^2-\beta^2}}dz-D_A-\int_{\sqrt{\beta^2+1}}^{\sqrt{\beta^2+4}}\frac{erfc(\gamma\cdot z)}{\sqrt{z^2-\beta^2}}dz-D_B\right] \tag{7}$$

In the above expression, $\gamma=1\Big/\left(2\sqrt{Fo_H}\right)$, β is the radial distance made dimensionless by the BHE length *H*, and D_A e D_B are equal to:

$$D_A=\int_{\beta}^{\sqrt{\beta^2+1}}erfc(\gamma\cdot z)\,dz=\sqrt{\beta^2+1}\cdot erfc\left(\gamma\cdot\sqrt{\beta^2+1}\right)-\beta\cdot erfc(\gamma\cdot\beta)-\frac{e^{-\gamma^2(\beta^2+1)}-e^{-\gamma^2\beta^2}}{\beta\sqrt{\pi}}$$

$$D_B=\sqrt{\beta^2+1}\cdot erfc\left(\gamma\cdot\sqrt{\beta^2+1}\right)-0.5\left[\beta\cdot erfc(\gamma\cdot\beta)+\sqrt{\beta^2+4}\cdot erfc\left(\gamma\cdot\sqrt{\beta^2+4}\right)\right]+$$
$$-\frac{e^{-\gamma^2(\beta^2+1)}-0.5\left[e^{-\gamma^2\beta^2}+e^{-\gamma^2(\beta^2+4)}\right]}{\beta\sqrt{\pi}}$$

Claesson and Javed (2011) reformulated the FLS theory according to new expressions where the distance *D* of the line source from the ground top surface (buried depth) can be taken into account:

$$\Gamma_{FLS\ ave}(r,\tau)=\frac{1}{2}\cdot\left[\int_{\sqrt{1/4Fo_H}}^{\infty}\exp\left[-(r/H)^2z^2\right]\cdot\frac{Y(z,D/H\cdot z)}{z^2}dz\right] \tag{8}$$

$$Y(x,y)=2ierf(x)+2ierf(x+2y)-ierf(2x+2y)-ierf(2y) \tag{9}$$

$$ierf(U)=\int_o^U erf(v)dv=U\,erf(U)-\frac{1}{\sqrt{\pi}}\left(1-e^{-U^2}\right) \tag{10}$$

The Infinite Cylindrical Source model (ICS) refers to a geometry in which the source is an infinitely long hollow cylindrical surface. The ICS case was analytically solved by Carlslaw and Jaeger (1947), either considering the heat rate boundary condition or the temperature one. Solving these problems they provided the *G* and *F* solutions, as described below:

$$\Gamma_{ICS\ Q}(r,\tau)=2\pi\cdot G\left(Fo_{rcyl},p=\frac{r}{r_{cyl}}\right)=$$
$$=\frac{2}{\pi}\int_0^{\infty}\frac{e^{-\beta^2\cdot Fo_{rcyl}}-1}{J_1^2(\beta)+Y_1^2(\beta)}\left[J_0(p\beta)Y_1(\beta)-J_1(\beta)Y_0(p\beta)\right]\frac{1}{\beta^2}d\beta \tag{11}$$

$$\Gamma_{ICS\ T}(r,\tau)=\frac{2\pi}{F\left(Fo_{rcyl}\right)}=\frac{\pi^2/4}{\int_0^{\infty}\frac{e^{-\beta^2\cdot Fo_{rcyl}}}{J_0^2(\beta)+Y_0^2(\beta)}\frac{1}{\beta}d\beta} \tag{12}$$

where J_0, J_1, Y_0, Y_1 are Bessel functions of the zeroth and first order, respectively.
Later Ingersoll et al. (1954) provided tabulated values of the related solutions.
According to Fossa (2017), the ICS solution can be approximated, with an error below 1%, using the following Equation:

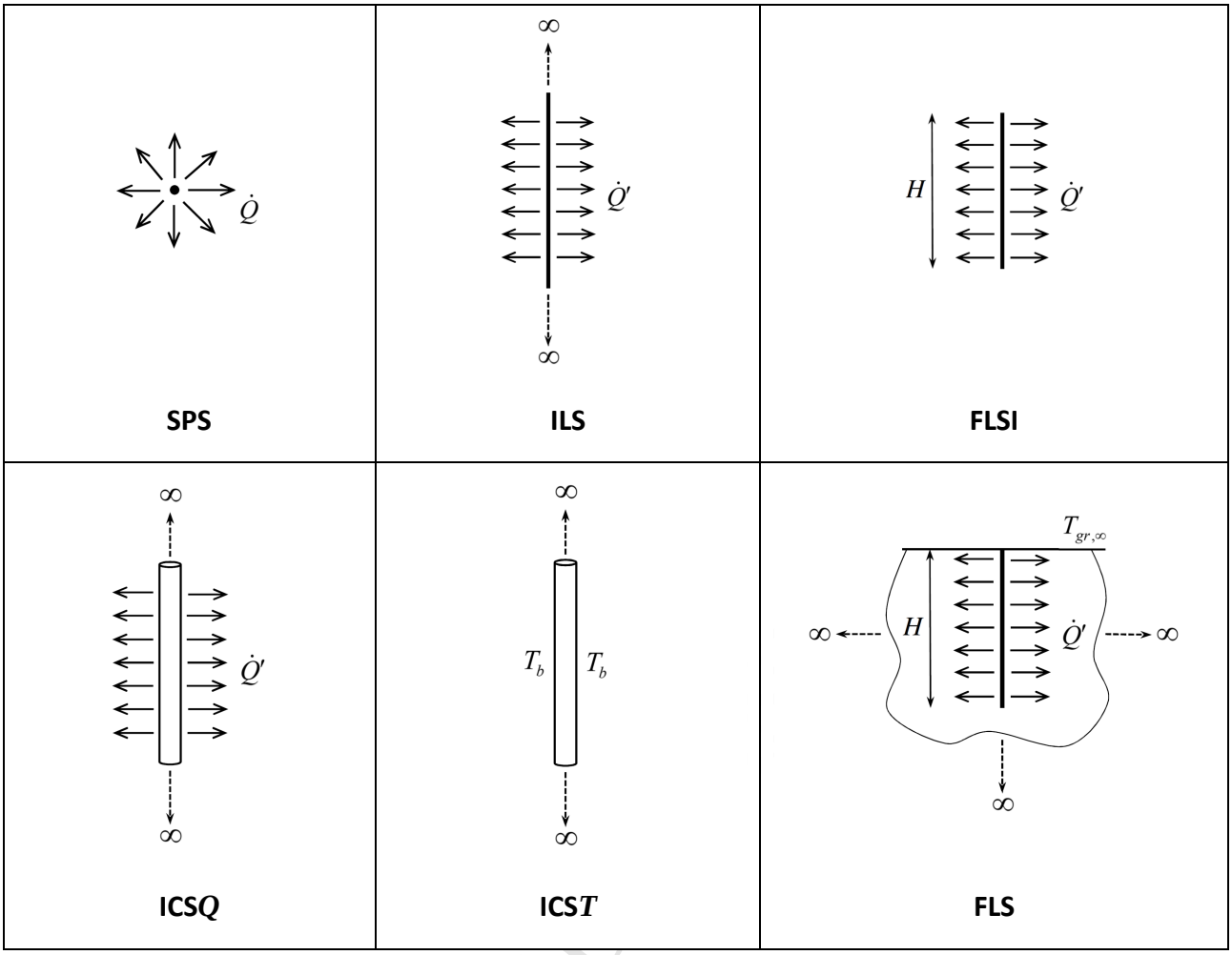

Table 1. Point, Line and Cylindrical heat sources: geometry and boundary conditions.

$$\Gamma_{ICS\,Q}(r = r_{cyl}, \tau) = 2\pi \cdot \left[\sum_{j=0}^{6} c_j Log^{j}{}_{10}(Fo_{rcyl}) \right] \quad (13)$$

where

c_0 = 1.2777 E-1 c_1 = 1.0812 E-1 c_2 = 3.0207 E-2 c_3 = - 2.30337 E-3

c_4 = - 1.4459 E-3 c_5 = 3.6415 E-4 c_6 = - 2.4889 E-5

2.2 Analytical solutions for Helix Heat Exchangers (HHE)

Ground heat exchangers as short energy piles cannot be modeled as infinite sources or linear ones because of their low aspect ratio (reduced depth with respect to classical Borehole Heat Exchangers, BHE) and relevant contribution of the thermal capacity of the inner cylindrical volume. For these reasons new specific models are needed. In this section cylinder, ring and helix heat sources are considered according to the geometries described in Table 2.

In recent years, a Chinese research group (Man et al. 2010-2011, Cui et al. 2011) has derived different analytical models to represent the ground response to the presence of HHEs. The models, derived from the application of the Green's function method, are the Infinite and Finite Solid Cylindrical source model, the Infinite and Finite Ring Source model, the Infinite and Finite Spiral Source model.

In the following, the models are briefly illustrated. For the finite length models, the ground is assumed to be a semi-infinite medium and the temperature of the ground surface is kept constant and equal to $T_{gr,\infty}$. For all the models, a constant heat transfer rate per unit of borehole length is considered as imposed boundary condition.

The Infinite Solid Cylindrical Source (ISCS) model has been proposed by Man et al. (2010) to improve the existing "hollow" cylindrical counterparts (e.g. the ICS model) taking into account the heat capacity of the inner cylindrical volume. The solution can be obtained as follows:

$$\Gamma_{ISCS}(r,\tau) = -\frac{1}{2}\cdot\int_0^{\pi}\frac{1}{\pi}\cdot E_i\left(-\frac{r^2+{r_{pile}}^2-2r\cdot r_{pile}\cos\varphi}{4a\tau}\right)d\varphi \tag{14}$$

Man et al. (2010) elaborated also a Finite Solid Cylindrical Source (FSCS) model that considers a cylindrical source with depth *H*. The analytical solution is:

$$\Gamma_{FSCS}(r,z,\tau) = \frac{1}{4}\cdot\int_0^{\tau}\frac{1}{\tau}\cdot I_0\left[\frac{r\cdot r_{pile}}{2a\tau}\right]\cdot\exp\left[-\frac{r^2+{r_{pile}}^2}{4a\tau}\right]\cdot\left\{erf\left[\frac{H-z}{2\sqrt{a\tau}}\right]+2erf\left[\frac{z}{2\sqrt{a\tau}}\right]-erf\left[\frac{H+z}{2\sqrt{a\tau}}\right]\right\}d\tau \tag{15}$$

Cui et al. (2011) developed the Infinite Ring Source (IRS) model considering the heat source composed by an infinite series of rings stacked around a vertical axis. In this way it is possible to take into account the discontinuities of real helix sources and the impact of the coil pitch *p*. The proposed analytical solution results:

$$\Gamma_{IRS}(r,z,\tau) = \frac{p/r_{pile}}{4\sqrt{\pi}}\cdot\sum_{n=0}^{\infty}\int_0^{Fo}\frac{1}{{Fo_{rpile}}^{3/2}}\cdot I_0\left[\frac{r/r_{pile}}{2Fo_{rpile}}\right]\cdot\exp\left[-\frac{\left(r/r_{pile}\right)^2+1}{4Fo_{rpile}}\right]\cdot \cdot\left\{\exp\left[-\frac{\left(\frac{z-n\cdot p-0.5\cdot p}{r_{pile}}\right)^2}{4Fo_{rpile}}\right]+\exp\left[-\frac{\left(\frac{z+n\cdot p+0.5\cdot p}{r_{pile}}\right)^2}{4Fo_{rpile}}\right]\right\}dFo_{rpile} \tag{16}$$

Cui et al. (2011) proposed also the Finite Ring Source (FRS) model, considering a cylindrical source with depth *H*, composed by *m* rings and they obtained the following expression:

$$\Gamma_{FRS}(r,z,\tau) = \frac{p/r_{pile}}{4\sqrt{\pi}}\cdot\int_0^{Fo}\frac{1}{{Fo_{rpile}}^{3/2}}\cdot I_0\left[\frac{r/r_{pile}}{2Fo_{rpile}}\right]\cdot\exp\left[-\frac{\left(r/r_{pile}\right)^2+1}{4Fo_{rpile}}\right]\cdot \cdot\sum_{n=0}^{m}\left\{\exp\left[-\frac{\left(\frac{z-n\cdot p-0.5\cdot p}{r_{pile}}\right)^2}{4Fo_{rpile}}\right]-\exp\left[-\frac{\left(\frac{z+n\cdot p+0.5\cdot p}{r_{pile}}\right)^2}{4Fo_{rpile}}\right]\right\}dFo_{rpile} \tag{17}$$

Man et al. (2011) refined the representation of the HHE introducing the spiral geometries. These models consider the coil pipe as a helix buried in the ground around a vertical axis with a fixed coil pitch *p*.
The Infinite Spiral Source (ISS) solution is:

$$\Gamma_{ISS}(r,\varphi,z,\tau)=\frac{p/r_{pile}}{8\cdot\pi\sqrt{\pi}}\cdot\int_0^{Fo}\frac{1}{Fo_{rpile}^{\ 3/2}}\cdot$$

$$\cdot\int_{-\infty}^{\infty}\exp\left[-\frac{\left(r/r_{pile}\right)^2+1-2\left(r/r_{pile}\right)\cdot\cos(\varphi-\varphi')+\left(\frac{z-p\cdot\varphi'/2\pi}{r_{pile}}\right)^2}{4\cdot Fo_{rpile}}\right]d\varphi'\cdot dFo_{rpile} \qquad (18)$$

The Finite Spiral Source (FSS) model considers a finite number of spiral coils equal to *m* and its analytical solution is:

$$\Gamma_{FSS}(r,\varphi,z,\tau)=\frac{p/r_{pile}}{8\cdot\pi\sqrt{\pi}}\cdot\int_0^{Fo}\frac{1}{Fo_{rpile}^{\ 3/2}}\cdot\exp\left[-\frac{\left(r/r_{pile}\right)^2+1}{4Fo_{rpile}}\right]\cdot$$

$$\cdot\int_0^{2\pi H/b}\exp\left[\frac{2\left(r/r_{pile}\right)\cdot\cos(\varphi-\varphi')}{4Fo_{rpile}}\right]\cdot\left\{\exp\left[-\frac{\left(\frac{z-p\cdot\varphi'/2\pi}{r_{pile}}\right)^2}{4Fo_{rpile}}\right]-\exp\left[-\frac{\left(\frac{z+p\cdot\varphi'/2\pi}{r_{pile}}\right)^2}{4Fo_{rpile}}\right]\right\}d\varphi'\cdot dFo_{rpile} \qquad (19)$$

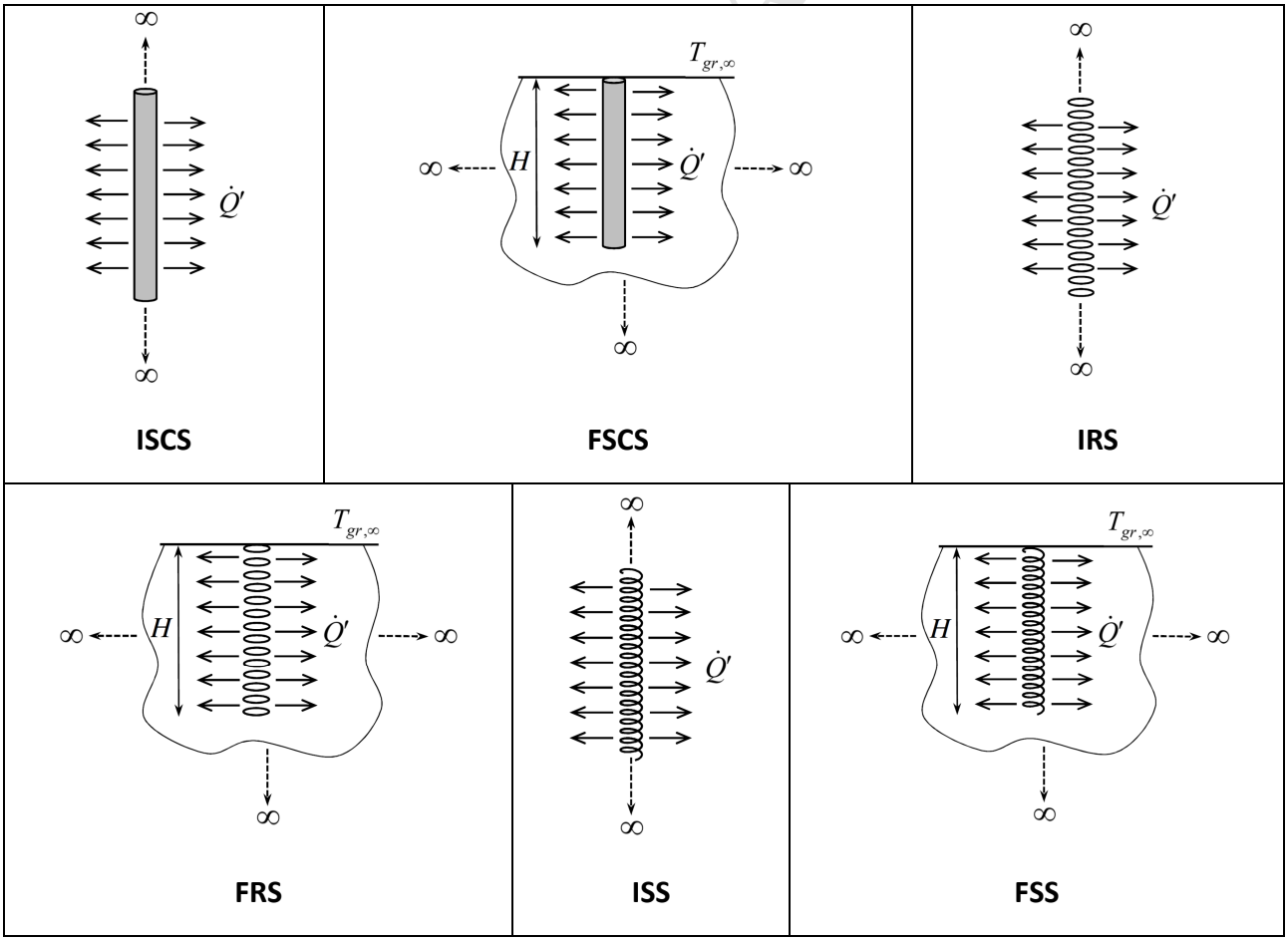

Table 2. Solid Cylinder, Ring and Helix heat sources: geometry and boundary conditions.

3. Present study method: the multiple point source model (MPS)

In this paper a semi-analytical method is presented, suitable to model any GHE geometry, irrespective of the piping shape and not relying on any specific symmetry condition. The model is based on the spatial superposition of the Single Point Source (SPS) solution (Eq.2). The sources are placed along a suitable contour to create the desired geometry including rings and helix coils.

In order to impose constant temperature at the ground surface, equal to the undisturbed one $T_{gr,\infty}$, the image source approach is applied and a opposite strength heat transfer rate is applied to all the image sources.

For each position *j* of the ground domain, the overall temperature excess with respect to the undisturbed value $T_{gr,\infty}$ can be evaluated at each instant as superposition of the effects induced by all the $N_{sources}$ point sources, including the image ones:

$$T_j(\tau) - T_{gr,\infty} = \sum_{i=1}^{Nsources} T_{i,j}(\tau) - T_{gr,\infty} \tag{20}$$

Recalling the solution for the Single Point Source (Eq.2) one obtains:

$$T_j(\tau) - T_{gr,\infty} = \frac{\dot{Q}}{4\pi k_{gr}} \sum_{i=1}^{Nsources} \frac{1}{r_{i,j}} erfc\left(\frac{1}{2\sqrt{(Fo_r)_{i,j}}}\right) \tag{21}$$

Finally, the average temperature excess related to all the *j* ground positions taken into account can be evaluated as follows:

$$\bar{T}(\tau) - T_{gr,\infty} = \frac{1}{N_{positions}} \sum_{j=1}^{Npositions} T_j(\tau) - T_{gr,\infty} \tag{22}$$

In the application of the suggested method, a fundamental issue is the definition of the minimum number of point sources to be superposed to properly represent any curved line constituting a heat source. This problem is equivalent to assess the maximum allowed distance between the single sources. This distance (PS to PS distance or grid size Δs) necessarily depends on another geometrical parameter, i.e. the distance of PS from neighbor evaluation point (EP).

Considering Figure 1, single point sources are placed on a generic curved line at a distance equal to Δs. The Temperature Response Factor is evaluated at a distance r_b from the source, normal to the curved line. In this original way, the ground response is evaluated at the virtual location of the pipe boundary and no "grout type" heat resistance has to be inserted in the model. The selection of the PS density along the path describing the pipe arrangement has to be done while reaching a tradeoff between discretization accuracy and computational time saving. For this reason, a series of preliminary calculations and comparisons with respect to reference analytical solutions has been performed to assess the best discretization parameter $\Delta s/r_b$.

First, the analysis has been carried out for a linear geometry, to compare the results obtained with the multiple point source (MPS) model with the results from the FLS analytical solution.

Figure 2 shows the comparison between the temperature response factor from the FLS solution ($r_b/H = 0.001$) and those obtained with the MPS model for different values of $\Delta s/r_b$. As can be observed, the MPS solution approaches the reference FLS one when the discretization parameter $\Delta s/r_b$ is of the order of the unit (Fossa 2017).

A similar analysis has been applied to a helix heat exchanger approximated as a series of rings, with radius r_{pile}, total high *H* and pitch *p*, according to Figure 3 and Table 3. The temperature field is evaluated at a distance r_b from the sources. The rings are modeled by the superposition of single point sources, each with an applied heat transfer rate equal to $\dot{Q}_{PS}$. The number of the PS for each ring defines the parameter $\Delta s/r_b$.

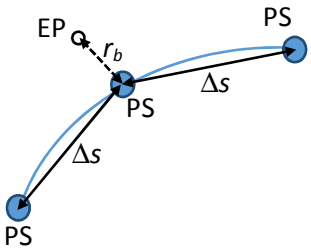

Figure 1. Discretization scheme for a generic curved line in order to apply the MPS method.

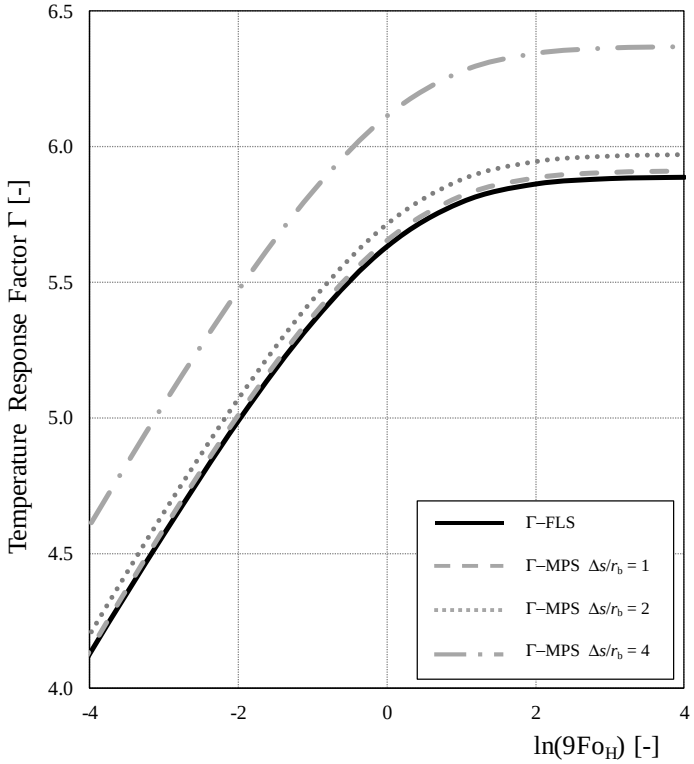

Figure 2. Comparison of reference FLS results (r_b/H = 0.001) with MPS superposition solutions for different $\Delta s/r_b$.

The evaluation of the Temperature Response Factor Γ for the HHE is carried out by increasing the number of PS for each ring, up to N_{PS} = 140, with a corresponding parameter $\Delta s/r_b$ = 1 (Table 4). Figure 4 represents the Γ functions for the different $\Delta s/r_b$ and shows that, increasing the number of PS and so decreasing the value of $\Delta s/r_b$, the different MPS profiles approach.

Table 3. HHE geometrical parameters.

H [m]	15
r_{pile} [m]	0.45
p [m]	0.5
r_b [m]	0.02

Table 4. Discretization parameters and average relative errors for ring heat exchangers.

N_{PS}	$\Delta s = 2 \cdot \pi \cdot r_{pile}/N_{PS}$	$\Delta s/r_b$	ε%
18	0.16	7.8	-
35	0.08	4	17.8%
70	0.04	2	6.1%
140	0.02	1	0.9%

To quantify the effect of the discretization parameter and compare the Γ functions obtained with increasing N_{PS}, it is possible to define an average relative error as:

$$\varepsilon\% = ave\left|\frac{\Gamma_i - \Gamma_{i+1}}{\Gamma_{i+1}}\right|\% \tag{23}$$

The calculated values are reported in Table 4 and show that, decreasing the parameter $\Delta s/r_b$ from 2 to 1 does not produce a relevant change in the Γ value, with a relative error equal to 0.9%. Therefore, it is possible to consider as general criterion the value $\Delta s/r_b = 2$, with a good compromise between accuracy and computational time savings.

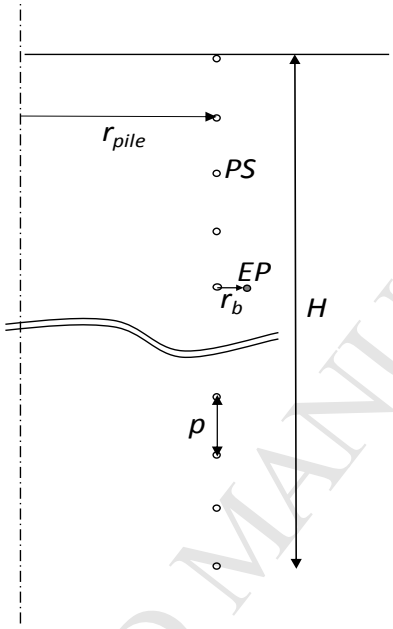

Figure 3. Sketch of a helix heat exchanger (HHE) approximated as a series of rings.

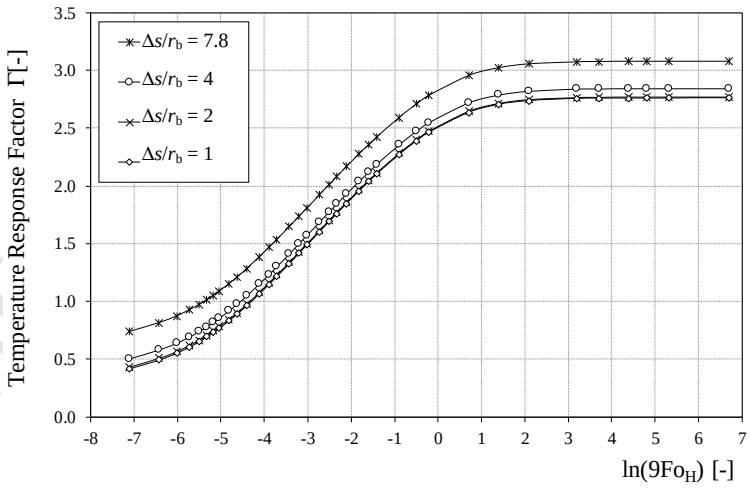

Figure 4. MPS method: effect of the discretization parameter $\Delta s/r_b$ on the evaluation of Γ functions for a ring heat exchanger.

To further validate the suggested method, the temperature response factor Γ obtained with the MPS method for the geometry represented in Figure 3 has been compared with literature analytical solutions.

In particular, the infinite and finite solid cylindrical source (ISCS and FSCS) and the infinite and finite ring source (IRS and FRS) solutions have been considered (Man et al. 2010, Cui et al. 2011).
In this case the Γ functions have been evaluated at r = 0.45 and for more vertical positions than the numbers of rings, i.e. 10 evaluation points for each pitch distance. For this reason, the Γ functions result in their asymptotic values are smaller than those showed in Figure 4.
At low Fo values, i.e. $\ln(9Fo_H)<-4$ (corresponding to $Fo_{rb}<2$), all the Γ functions have to match with the ILS trend. On the contrary, it is relevant to point out that the Γ values obtained with the IRS solution move slightly away. It is not clear if this behavior has to ascribed to the solver of the Matlab code used to solve Equation 16 or to some inefficiency of the analytic expression.
For higher Fo numbers, Figure 5 clearly confirms that the MPS method allows to find results that are in very good agreement with the corresponding ones from the analytical solutions, with an average relative error at the asymptote with respect to FSCS and FRS equal to 2.8% and 1.8%, respectively.
An additional comparison related to the present method predictions is shown in Figure 6. Here a FRS is considered and its geometrical parameters are H=15 m, r_{pile}=0.45 m, p=0.25 m. A 2-D Comsol FEM model has been built on purpose: a constant heat transfer rate condition has been imposed to ring external surface and the temperature field (in time and space) has been calculated. From the average temperature along rings at given distance (0.02 m), the TRF of the present heat source geometry has been inferred and compared with the corresponding solution by the present MPS model.

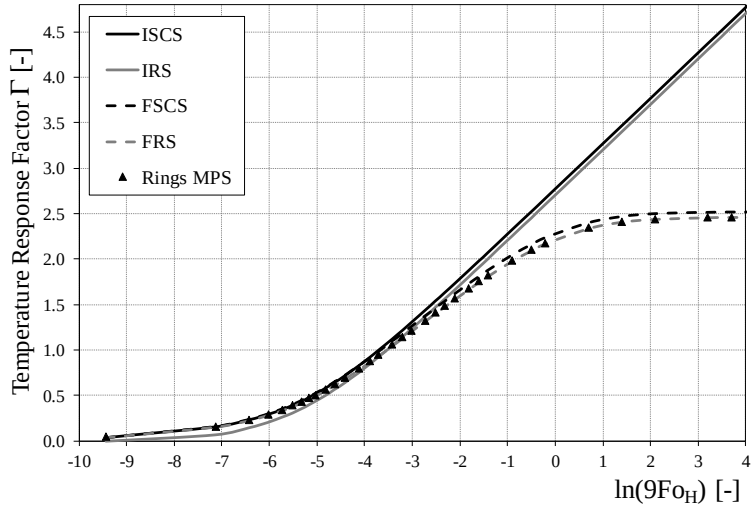

Figure 5. Comparison between the MPS results and analytical solutions.

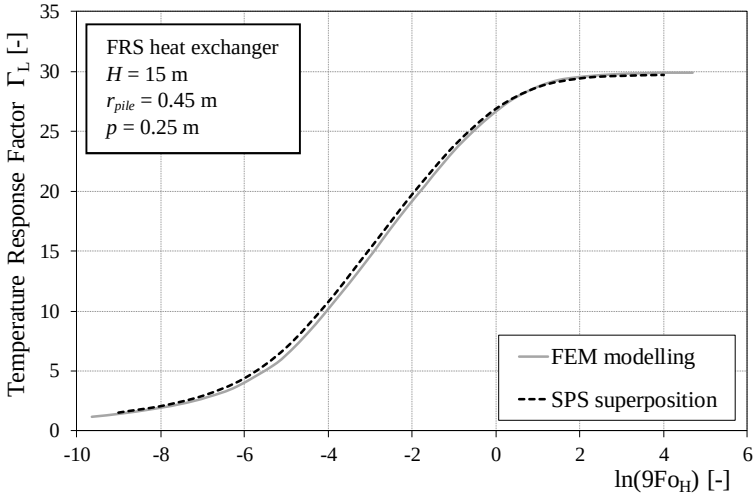

Figure 6. Comparison between the MPS results and FEM results in terms of Γ_L-function for a FRS heat exchanger. Geometrical parameters are given in figure legend.

In Figure 6 the temperature response factors Γ_L have been evaluated with respect to the heat transfer rate per unit helix length ($\dot{Q}'_L$) and not per unit pile depth ($\dot{Q}'$):

$$\Gamma_L = 2\pi k_{gr} \frac{T - T_{gr,\infty}}{\dot{Q}'_L} = \Gamma \cdot \frac{H}{L} \tag{24}$$

Again, as can be easily noticed, the agreement of the present method results with the FEM ones is very good (average difference 2.5%) at both the early part of the transient response and in the late period up to the asymptotic trend.

4. Results

The great advantage of the MPS method is that it allows generating heat sources of any shape, thus offering a terrific flexibility.

In geothermal pile applications, it is possible that the piping is arranged not as a spiral around the foundation pile but as a series of vertical pipes connected through U bends at top and bottom of a cylindrical volume (Figure 7). Even the vertical pipe arrangement is easier in terms of installation and probably safer with reference to concrete coverage on steel cage, some companies also propose helical pipes. The MPS method has been applied to generate the temperature response factor Γ for the above geometries and the results are compared to each other.

In the two different cases, Γ is evaluated at the same distance r_b from the sources, considering the same equal heat transfer rate $\dot{Q}$ for all the sources and setting the discretization parameter $\Delta s/r_b = 2$ to define the number of PS.

Finally, both geometries have nearly equal total pipe length L:

$$L = L_{rings} \cong L_{vertical\ pipes} \tag{25}$$

with:

$$L_{rings} = 2\pi \cdot r_{pile} \cdot \frac{H}{p} \qquad \text{and} \qquad L_{vertical\ pipes} = N_{legs} \cdot H + 2\pi \cdot r_{pile} \tag{26}$$

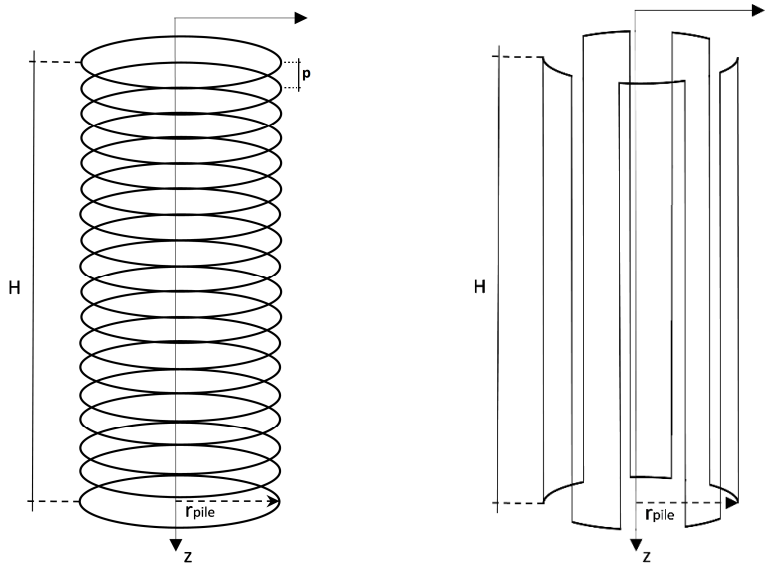

Figure 7. MPS method applications: rings and vertical pipe arrangements for geothermal piles.

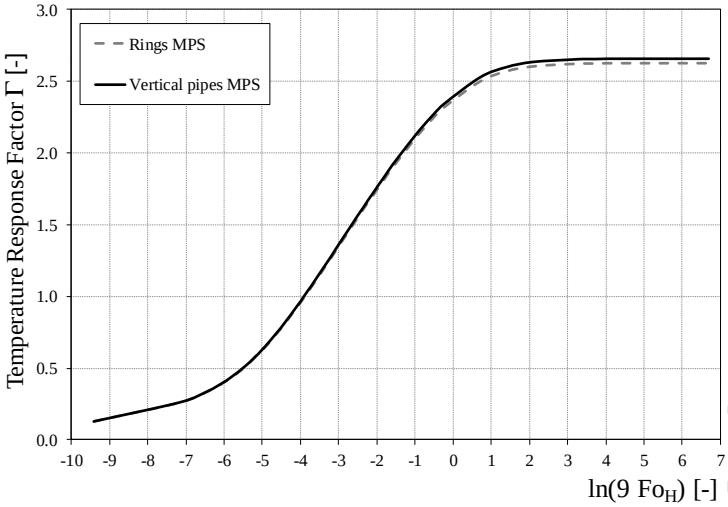

Figure 8. MPS results: comparison between rings and vertical pipe geometry.

The rings configuration has a coil pitch $p = 0.28$ m whereas the vertical pipes configuration considers a number of legs equal to 10. Thus, the total pipe length L for both geometries is nearly equal to 150 m.

Figure 8 shows the comparison between the two different Γ functions obtained with the MPS method. At small Fo_H ($\ln(9\ Fo_H) < -1$), the two curves reveal a very good agreement because, at the beginning, each point source cannot perceive the influence induced by the presence of the others. As a consequence, at a distance equal to r_b from PS, the response of the ground is nearly the same as for a single point source (SPS).

On the contrary, for high Fo_H, the effects of the other PS become relevant, and the shape of the two energy pile geometries induces slightly different response in the ground (with an asymptotic relative difference of nearly 1%).

5. Conclusions

For ground coupled heat pumps (GCHP), the use of vertical ground heat exchangers associated to the foundation structures of the building (energy piles) is a very interesting and promising technique. In this type of installation, the pipes are frequently arranged as helix heat exchangers (HHE) around the pile or as a series of vertical pipes connected through U bends at top and bottom of the cylindrical volume.

In recent years, some analytical solutions have been proposed in literature to analyze the energy piles. Unfortunately, they are complicated to be used and strictly associated to a particular geometry, i.e. a particular shape of the pipes arrangement around the pile.

In this paper, a new semi-analytical approach (Multiple Point Source method) has been proposed. The algorithm is based on the spatial superposition of the analytical solutions related to a system of single point sources arranged along a path describing the pipe shape. After an extensive analysis on the sources discretization, the method has been validated against analytical methods for a helix heat exchanger approximated as a series of rings with a fixed pitch. In particular, the ground response obtained with the MPS method has been compared with the analytical solutions of the Finite Solid Cylindrical Source model and the Finite Ring Source model with a very good agreement (average relative error equal to 2.8% and 1.8%, respectively). A very good agreement has also been obtained from the comparison with FEM simulations of a finite ring heat exchanger.

The proposed method is simply to use, effective and very flexible to be applied to other geometries, i.e. other pipes arrangements around the pile. As an example, the paper compares the ring coil

configuration with a series of vertical pipes connected through U bends at top and bottom of a cylindrical volume. Future investigations will be devoted to the application of the present method to sensitivity analyses on helix pitch effects.

Nomenclature

a	Thermal diffusivity [m^2/s];
E_1	Exponential Integral function [-]
erf	Error function [-];
Fo_r	Fourier number based on the radius r [-];
Fo_H	Fourier number based on the depth H [-];
H	Pile depth [m]
I_0	Modified Bessel function of the zero order [-];
J_0, J_1	Bessel Function of the first kind of zero and one order [-];
Y_0, Y_1	Bessel Function of the second kind of zero and one order [-];
k	Thermal conductivity [W/m K]
L	Total pipe length [m]
m	Number of rings [-]
p	Pitch [m];
$\dot{Q}$	Heat transfer rate [W];
$\dot{Q}$	Heat transfer rate per unit length [W/m];
r	Radial coordinate [m];
Δs	Distance between SPS [m]
T	Temperature [K];
$T_{gr,\infty}$	Undisturbed (initial) ground temperature [K];
z	Axial coordinate [m]

Greeks

β	Dimensionless radial distance (r/H) [-]
ε	Average relative error [%]
Γ	Temperature Response Factor [-]
φ	Angular coordinate
τ	Time [s];

Subscripts

b	Referred to the point at which the Γ is evaluated
gr	Referred to ground
$pile$	Referred to pile

References

- Abramovitz M., I. Stegun (1964), Handbook of mathematical functions with formulas, graphs, and mathematical tables, National Bureau of Standards, 228–233.
- Bernier M.A., P. Pinel, R. Labib, R. Paillot (2004), A multiple load aggregation algorithm for annual hourly simulations of GCHP systems, International Journal of Heating, Ventilating, Air-Conditioning and Refrigeration Research 10, 471–488.
- Carslaw H.S., J.C. Jaeger (1947), Conduction of Heat in Solids, Claremore Press, Oxford, UK.

- Claesson J., S. Javed (2011), An analytical method to calculate borehole fluid temperatures for time-scales from minutes to decades, ASHRAE Trans. 117(2), 279–288.
- Cui P., X. Li, Y. Man, Z. Fang (2011), Heat transfer analysis of pile geothermal heat exchangers with spiral coils, Applied Energy 88, 4113-4119.
- Eskilson P. (1987), Thermal Analysis of Heat Extraction Boreholes. Ph.D. Thesis, Lund University of Technology, Sweden.
- Fossa M. (2017), Correct design of vertical borehole heat exchanger systems through the improvement of the ASHRAE method, Science and Technology for the Built Environment 23(7), 1080-1089.
- Ghasemi-Fare O., P.Basu (2016), Predictive assessment of heat exchange performance of geothermal piles, Renewable Energy 86, 1178-1196.
- Go G.H., S.R. Lee, H.B. Kang, S. Yoon, M.J. Kim (2015), A novel hybrid design algorithm for spiral coil energy piles that considers groundwater advection, Applied Thermal Eng. 78, 196-208.
- Holmberg H., J. Acuna, E. Næss, O.K. Sønju, (2016), Thermal evaluation of coaxial deep borehole heat exchangers, Renewable Energy 97, 65-76.
- Ingersoll L.R., O.J. Zobel, A.C. Ingersoll (1954), Heat Conduction with Engineering, Geological, and other Applications, McGraw-Hill, New York.
- Jelušič P., B. Žlender (2018), Determining optimal designs for conventional and geothermal energy piles, Renewable Energy, Available online 9 August 2018, https://doi.org/10.1016/j.renene.2018.08.016.
- Lamarche L., B. Beauchamp (2007), A new contribution to the finite line-source model for geothermal boreholes, Energy and Buildings 39, 188–198.
- Man Y., H. Yang, N. Diao, J. Liu, Z. Fang (2010), A new model and analytical solutions for borehole and pile ground heat exchangers, Int. J. Heat Mass Transfer 53, 2593-2601.
- Man Y., H. Yang, N. Diao, P. Cui, L. Lu, Z. Fang (2011), Development of spiral heat source model for novel pile ground heat exchangers, HVAC&R Research 17, 1075-1088.
- Moch X., M. Palomares, F. Claudon, B. Souyri (2014), Geothermal helical heat exchangers: Comparison and use of two-dimensional axisymmetric models, Applied Thermal Eng. 73, 689-696.
- Priarone A., M. Fossa (2016), Temperature response factors at different boundary conditions for modelling the single borehole heat exchanger, Applied Thermal Engineering 103, 934–944.
- Rabin Y., E. Korin (1996), Thermal analysis of helical heat exchanger for ground thermal energy storage in arid zones, Int. J. Heat mass Transfer 39, 1051-1065.
- Yavuzturk C., J.D. Spitler (1999), A short time step response factor model for vertical ground loop heat exchangers, ASHRAE Transactions 105, 475–485.
- Zarrella A., G. Emmi, M. DeCarli (2015), Analysis of operating modes of a ground source heat pump with short helical heat exchangers, Energy Conversion and Management 97, 351-361.
- Zeng H.Y., N.R. Diao, Z.H. Fang (2002), A finite line-source model for boreholes in geothermal heat exchangers, Heat Transfer-Asian Research 31, 558-567.

- Geothermal piles are heat exchangers integrated in the foundations of the buildings
- They have low aspect ratio and high heat capacity in the inner cylindrical volume
- It is not possible to use classical analytical solutions
- A new semi-analytical method called multiple point sources (MPS) is proposed
- The method has been validated against analytical and FEM models